

Article

## Poly- $\beta$ -Cyclodextrin Functionalized Nanocellulose for Efficient Removal of Endocrine Disrupting Chemicals

Humendra Poudel<sup>1</sup>, Ambar B. RanguMagar<sup>2,\*</sup>, Ahona Ghosh<sup>1</sup>,  
Shawn E. Bourdo<sup>3</sup>, Fumiya Watanabe<sup>3</sup>, Daoyuan Wang<sup>4</sup>, Anindya Ghosh<sup>1,\*</sup>

<sup>1</sup> Department of Chemistry, University of Arkansas at Little Rock, 2801 South University Avenue, Little Rock, AR 72204, USA

<sup>2</sup> Department of Chemistry, Philander Smith University, Little Rock, AR 72202, USA

<sup>3</sup> Center for Integrative Nanotechnology Sciences, University of Arkansas at Little Rock, 2801 South University Avenue, Little Rock, AR 72204, USA

<sup>4</sup> Department of Chemistry and Physics, University of Arkansas at Pine Bluff, Pine Bluff, AR 71601, USA

\* Correspondence: Ambar B. RanguMagar, Email: arangumagar@philander.edu; Anindya Ghosh, Email: axghosh@ualr.edu.

### ABSTRACT

This study aims to develop a highly efficient adsorbent specifically designed to remove targeted organic pollutants, focusing on endocrine disruptors. The pollutants of interest included bisphenol S (BPS), triclosan (TCS), and 2,4,6-trichlorophenol (TCP), which are commonly found in aqueous solutions. The surface of nanocellulose (NC) was modified with poly- $\beta$ -cyclodextrin (p- $\beta$ CD) using epichlorohydrin as a cross-linker. The modified NC-p- $\beta$ CD adsorbent exhibited remarkable adsorption performance due to the inclusion properties of  $\beta$ -cyclodextrin ( $\beta$ CD) and the advantages of NC. Comprehensive characterization techniques, including Fourier Transform Infrared Spectroscopy (FTIR), Nuclear Magnetic Resonance (NMR) Spectroscopy, Scanning Electron Microscopy (SEM), Thermogravimetric Analysis (TGA), and Energy Dispersive X-ray Spectroscopy (EDS) confirmed the successful modification and provided insights into the structural features of p- $\beta$ CD and NC-p- $\beta$ CD. The percentage removal of the target pollutants was quantified using UV-visible spectroscopy, and their adsorption kinetics were studied. The NC-p- $\beta$ CD demonstrated impressive removal efficiencies with maximum cumulative percentages of 28% for BPS, 74% for TCS, and 58% for TCP. The adsorption process followed Langmuir adsorption kinetics, suggesting monolayer adsorption on a homogeneous surface. This study presents a promising adsorbent by modifying NC with p- $\beta$ CD to remove organic pollutants effectively. The findings contribute to developing sustainable water treatment methods using NC-based adsorbents.

**KEYWORDS:** nanocellulose; endocrine-disrupting chemicals; bisphenol S;  $\beta$ -cyclodextrin; triclosan; 2,4,6-trichlorophenol

### Open Access

Received: 05 July 2023

Accepted: 24 August 2023

Published: 31 August 2023

Copyright © 2023 by the author(s). Licensee Hapres, London, United Kingdom. This is an open access article distributed under the terms and conditions of [Creative Commons Attribution 4.0 International License](https://creativecommons.org/licenses/by/4.0/).

## INTRODUCTION

Water, an indispensable component of life [1], faces a significant challenge of pollution caused by various harmful and toxic contaminants due to their inappropriate disposal [2,3]. The presence of these contaminants in water has raised serious concerns due to their detrimental impact on human health and the environment [4,5]. These contaminants can be broadly classified as organic and inorganic impurities [6,7]. The organic pollutants commonly found in water include dyes, pharmaceuticals, phenolic compounds, surfactants, pesticides, and petroleum, while inorganic contaminants comprise arsenic, fluorides, and heavy metals [8,9]. Exposure to certain organic pollutants such as bisphenol S (BPS), bisphenol A (BPA), triclosan (TCS), and chlorinated phenols such as 2,4,6-trichlorophenol (TCP) (Figure 1) can lead to various health problems, including breast cancer, kidney damage, and endocrine disruptions [10,11]. Particularly, endocrine-disrupting chemicals have posed a serious threat to us and other living objects in nature. Endocrine-disrupting chemicals mimic, function, and block any hormones in living systems, disrupting the natural processes of the endocrine systems [12]. Such disruptions may cause serious health issues and abnormalities in vertebrates, including humans [13]. Endocrine-disrupting chemicals can be either synthetic or natural compounds [14]. Over 1000 chemicals are known to us as endocrine-disrupting chemicals [15]. This manuscript deals with a simple removal technique for some endocrine-disrupting chemicals.

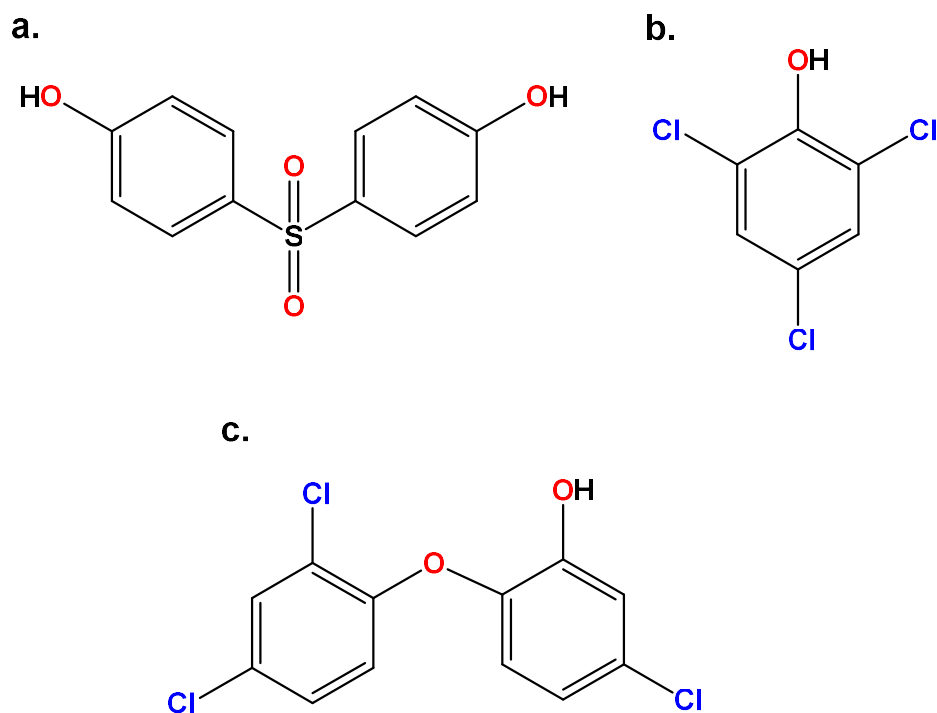


**Figure 1.** Chemical structures of (a) bisphenol S (BPS), (b) 2,4,6-trichlorophenol (TCP), and (c) triclosan (TCS).

BPS is predominantly present in the modern world in the form of plastics [16]. It has been detected in various aquatic bodies like rivers, lakes, and oceans [16]. Notably, studies have reported maximum BPS concentrations of 0.14 µg/L in the Pearl River (China) and 7.2 µg/L in Indian Rivers in 2016 [17,18]. Furthermore, BPS has even been identified in pristine environments like the Arctic [19].

BPS is an epoxy resin compound containing two hydroxyphenyl groups [20]. It is commonly employed in various applications such as packaging for baby formula, baby bottles, dental implants, personal care products (e.g., makeup, lotion, toothpaste), and meat products, owing to its heat tolerance and high photo-resistance [21–24]. However, despite its numerous advantages, BPS can give rise to severe health issues, including endocrine disruption, upon exposure to the human body [25]. Exposure to BPS can occur through microwaving food, and if the monolayer of plastic is decomposed by chemicals or other means, food can become contaminated by BPS [26]. Additionally, bisphenol polymers, including BPS, can enter the body through water [27,28]. Notably, BPS has been detected in urine samples of approximately 81% of Asian and American individuals, with an average concentration of 2.6 nM [29].

Research shows that BPS changes the aromatase expression of the estrogen pathway due to its ability to mimic this hormone and interact with specific receptors, including estrogen, androgen, and serum proteins [30]. Furthermore, an *in vivo* study has demonstrated that BPS can induce adverse effects such as reproductive dysfunction at low doses and even depressive symptoms at high doses [31]. Additionally, evidence suggests that BPS can impact the nervous system [32] and contribute to various health issues, including breast cancer, metabolic disorders, DNA damage, and cardiovascular diseases [33–35]. Given these concerns, the removal of BPS from water sources is of utmost importance. Filtration has been identified as one of the simplest and most effective methods for eliminating BPS from water [36].

Another notable endocrine-disrupting chemical is TCS, previously used as an antimicrobial agent in manufacturing soaps, detergents, cosmetics, textiles, toothpaste, and food packaging [37]. However, exposure to TCS can be toxic to humans, leading to potential endocrine disruption, cancer, and thyroid disease [38]. As a result of its adverse effects, the Food and Drug Administration (FDA) decided to prohibit the use of TCS in soap products in 2016. However, it is still permitted for use in toothpaste and mouthwash [38].

Various methods commonly employed to remove TCS include ozonation, oxidation, adsorption, and membrane separation [39]. Several previous research has already been conducted in this area [40] to remove TCS. For instance, Kong et al. utilized polymer-functionalized magnetic iron oxides in the adsorption method to remove TCS from wastewater [41]. However, this method has been associated with relatively high costs [41]. Consequently, there is a need for an alternative approach, and one

promising candidate is NC-p- $\beta$ CD, which offers the advantages of being low in cost and easy to prepare.

TCP, also known as 2,4,6-trichlorophenol, is a prevalent phenolic pollutant characterized by the presence of three chlorine atoms attached to the phenolic ring at positions 2, 4, and 6 [41]. It is commonly encountered in industrial wastewater originating from diverse sectors such as coke, petroleum, pesticide, insecticide, pharmaceuticals, paper, and food industries [42]. Due to its high toxicity to humans and aquatic life, even at low concentrations, TCP poses a significant risk, potentially leading to carcinogenic and mutagenic diseases [43]. Consequently, the removal of TCP is of utmost importance, and various methods are commonly employed for this purpose, including photocatalytic degradation, microbial degradation, oxidation, ion exchange, and filtration [42]. Among these methods, filtration, specifically adsorption, has proven to be one of the most effective techniques for removing TCP [42]. Activated carbon is widely used as an adsorbent for TCP removal in granular and powdered forms. However, it should be noted that activated carbon can be expensive [44].

Prior research indicates that adsorbent materials, namely nano-zeolite, biochar, and activated carbon, have demonstrated effective utility in eliminating BPS, TCS, and TCP, respectively. Nonetheless, these materials exhibit certain limitations, as outlined in Table 1.

**Table 1.** Various adsorbent materials for phenolic impurity removal using adsorption techniques and their drawbacks.

Impurities	Adsorbent Materials	Disadvantages
Bisphenol S	Nano-zeolite	Non-recyclable, highcost, and environmental pollution [45]
	Carbon nanotubes	Preparation process complex [46]
Trichlosan	Biochar	Enviromental pollution [47]
	Carbon black	Low adsorption capacity [48]
	Graphene oxide	Environmental pollution [49]
2,4,6-trichlorophenol	Activated carbon	High cost and environmental pollution [50]
	Mango seed and sodium alginate beads	Time consuming process [51]

In this work, poly- $\beta$ -cyclodextrin (p- $\beta$ CD) was prepared by polymerization of  $\beta$ -cyclodextrin ( $\beta$ CD) and modified with nanocellulose (NC). The resulting modified polymer (NC-p- $\beta$ CD) was characterized by different characterization techniques such as FTIR spectroscopy, NMR Spectroscopy, SEM, TGA, and EDS. The schematic diagram for the modification of NC with p- $\beta$ CD is shown in Figure 2.

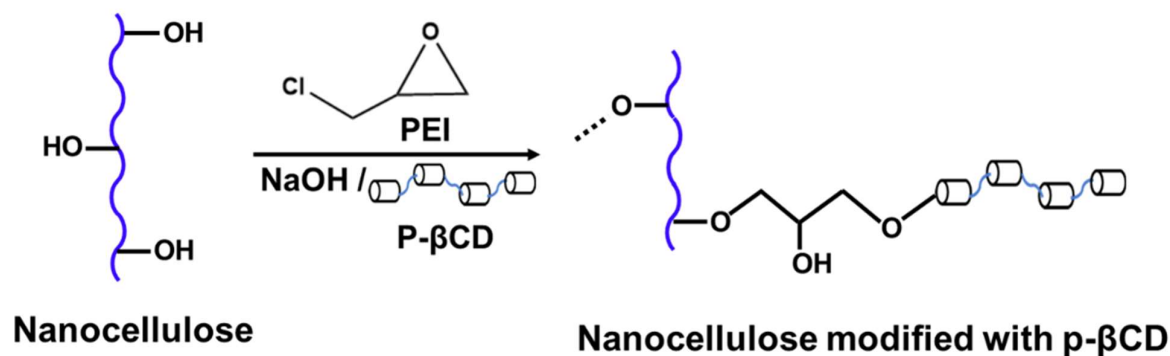


**Figure 2.** Schematic diagram for the modification of NC with p-βCD.

The modified nanocellulose (NC-p-βCD) served as a filtration matrix for the removal of organic pollutants due to its high adsorbent capacity, small size, and specific surface area expansions. This is complemented by the inherent benefits of nanocellulose, encompassing eco-friendliness, easy modification and functionalization, renewability, thermal resilience, and cost-effectiveness [52–54]. The adsorption process is based on the concept that BPS, TCS, and TCP all are hydrophobic, and the inside ring of p-βCD is also hydrophobic so that these impurities can be entrapped inside p-βCD [55–57]. Its efficacy in water purification was determined mainly by filtering organic pollutants such as BPS, TCS, and TCP by varying the amount of adsorbents and pH. The percentage of cumulative impurities removal was increased with an increase in pH and amount of NC-p-βCD due to higher interactions between the impurities and adsorbents. To our current understanding, this marks the initial instance in which we have successfully created a biocompatible adsorbent matrix (NC-p-βCD) through covalent bonding and employed it to effectively eliminate endocrine disruptors such as BPS, TCS, and TCP.

## MATERIALS AND METHODS

### Materials

All reagents and solvents were obtained from commercial suppliers and used without further purification. Acetone  $\geq 99.5\%$ , absolute ethanol  $\geq 99.9\%$ , and isopropanol  $\geq 99.5\%$  were purchased from VWR BDH chemicals.  $\beta$ -cyclodextrin  $\geq 97.0\%$ , deionized water, epichlorohydrin (EPH)  $\geq 99.0\%$ , toluene  $\geq 99.8\%$ , sodium hydroxide (NaOH), hydrochloric acid (HCl), BPS  $\geq 98.0\%$ , TCS  $\geq 99.0\%$ , and TCP  $\geq 97.0\%$ , were obtained from Sigma-Aldrich, USA. NC was obtained from Blue Goose Biorefineries Inc., Canada. Nitrogen ( $N_2$ ) gas cylinders were obtained from Airgas company.

### Synthesis of Water-Soluble $\beta$ -Cyclodextrin Polymer

This synthesis was performed using the literature method [58] with slight modifications. Briefly, about 2 g of  $\beta$ CD was dissolved in 5 mL of 15% aqueous NaOH solution at 35 °C by stirring for 2 h. To the alkaline solution

of  $\beta$ CD, 2 mL of toluene was added with constant stirring, and the mixture was kept at the same temperature for 2 h. Next, 5 mol% of EPH (3.92 mL) was added to the mixture and kept for stirring for an additional 3 h. The resulting precipitate was neutralized to pH 7 by adding 2 M HCl solution dropwise. Once the reaction was complete, the solution was precipitated in isopropanol, and the solid was collected by filtration. The collected solid was dried in a freeze dryer, resulting in a powder form 1.92 g of p- $\beta$ CD.

### **Modification of Nanocellulose with p- $\beta$ -Cyclodextrin**

First, 20 mL of 8% NC was dissolved in 30 mL of distilled water (equivalent to 1.6 g of NC) in a round-bottom flask. The pH of the solution was adjusted to 9.5 by adding a 0.1 M NaOH solution. As a precaution, the mixture was purged with N<sub>2</sub> gas slowly. Subsequently, two equivalents of EPH (1.5 mL) were added, and the temperature was maintained at 50 °C for a duration of 2 h. After that, 1.6 g of p- $\beta$ CD was introduced into the reaction mixture, which was then stirred overnight. On the following day, the mixture underwent thorough washing with a copious amount of isopropanol, followed by drying in a freeze dryer, producing a powder form of 2.05 g of NC-p- $\beta$ CD.

### **Characterizations of Materials**

The NC, p- $\beta$ CD, and NC-p- $\beta$ CD were characterized by different spectroscopic and microscopic techniques such as FTIR Spectroscopy, NMR Spectroscopy, TGA, SEM, and EDS. The FTIR spectroscopy of the sample was conducted using a Nicolet 6700 Thermo-Scientific FTIR spectrometer equipped with a DLaTGS detector and an XT-KBr beam splitter. The spectra were recorded in the range of 400–4000 cm<sup>-1</sup>. The NMR spectroscopy was performed using a JEOL ECS-type nuclear magnetic resonance spectrometer with a frequency of 400 MHz. The weight loss of the NC and NC-p- $\beta$ CD compounds at different temperatures was measured using the TGA technique. The TGA analysis was successfully carried out using the Mettler Toledo thermogravimetric analyzer TGA/DSC3+. The surface morphology of the dried NC and NC-p- $\beta$ CD samples was examined using a JEOL scanning electron microscope (JSM 7000F) combined with an EDS system. The SEM images were captured at different magnifications to study the surface morphology of these samples. Furthermore, the concentrations of impurities were determined using a Perkin Elmer Inc. double-beam UV-Visible spectrophotometer covering the wavelength range of 200 to 700 nm.

### **Adsorption Techniques and Characterizations**

BPS, TCS, and TCP solutions were prepared at various pH levels ranging from 2 to 10. These solutions were individually passed through 100 milligrams (mg) of NC (control) and NC-p- $\beta$ CD samples to determine the percentage (%) removal of these impurities. The adsorption of impurities

was measured using UV-visible spectroscopy techniques. Additionally, the solutions were passed through varying amounts of adsorbent material (10 to 100 mg), and kinetic studies were conducted. Furthermore, to evaluate the recyclability of the NC-p- $\beta$ CD adsorbent, a test was performed over four consecutive cycles. In each cycle, a freshly prepared 4 mL of  $10^{-4}$  M concentration of BPS at pH 8.5 was passed through 100 mg of the adsorbent. After each cycle, the adsorbent was thoroughly washed three times using deionized (DI) water, and the sample was dried before introducing another 4 mL of  $10^{-4}$  M BPS solution for the subsequent cycle. This procedure allowed for effectively assessing the adsorbent's capability to remove BPS in a repeated usage scenario.

## RESULTS AND DISCUSSION

In this study, the characterization of  $\beta$ CD and p- $\beta$ CD was performed using FTIR and NMR spectroscopy. Supplementary Figure S1 in the Supporting Information displays the FTIR spectra of  $\beta$ CD and p- $\beta$ CD. The FTIR spectrum of  $\beta$ CD exhibits a broad peak at  $3300\text{ cm}^{-1}$  corresponding to hydroxyl (-OH) stretching and a prominent peak at  $2920\text{ cm}^{-1}$  attributed to C-H (symmetric and asymmetric stretching vibrations) bonds within the molecule. The presence of adsorbed water in  $\beta$ CD is indicated by the peak at  $1640\text{ cm}^{-1}$ , corresponding to H-OH deformation. The peaks observed at  $1150\text{ cm}^{-1}$  and  $1020\text{ cm}^{-1}$  also represent the C-H overtone and C-O stretching frequencies, respectively. The peak at  $1150\text{ cm}^{-1}$  also signifies the C-O-C vibration. These peaks align with values reported in the literature [59,60]. Following the polymerization of  $\beta$ CD, a slight shift in peaks is observed, but no new peaks emerge, as p- $\beta$ CD and  $\beta$ CD share similar functional groups. The shift from  $2920\text{ cm}^{-1}$  to  $2930\text{ cm}^{-1}$  is attributed to overlapping C-H peaks from EPH with  $\beta$ CD.

Supplementary Figure S2 (Supporting information) presents the  $^1\text{H-NMR}$  spectroscopy of p- $\beta$ CD in deuterium oxide ( $\text{D}_2\text{O}$ ) solvent. The  $^1\text{H-NMR}$  spectrum of p- $\beta$ CD exhibits six distinct peaks ranging from 1.1 ppm to 4.9 ppm. These peaks include a singlet at 4.9 ppm, a doublet at 3.5 ppm, another at 3.4, and a doublet at 1.1 ppm, corresponding to different proton environments of p- $\beta$ CD indicated in Supplementary Figure S2. Additionally, there are peaks at 3.7 ppm (singlet) and 3.8 ppm (triplet), which originate from the epichlorohydrin group. The observed peaks align perfectly with the different proton environments of p- $\beta$ CD, confirming the polymerization of  $\beta$ CD through epichlorohydrin as a cross-linker [59].

Supplementary Figure S3 in the Supporting Information illustrates the FTIR spectroscopy analysis of NC and p- $\beta$ CD-modified NC (NC-p- $\beta$ CD). In the FTIR spectrum of NC, a broad peak at  $3340\text{ cm}^{-1}$  corresponds to hydroxyl (-OH) stretching, while the intense peak at  $2910\text{ cm}^{-1}$  represents C-H stretching vibrations within the molecule. The H-OH deformation peak at  $1620\text{ cm}^{-1}$  in both NC and NC-p- $\beta$ CD persists after synthesis due to water molecule physisorption on the surfaces. The peak at  $1160\text{ cm}^{-1}$  in NC-p- $\beta$ CD also signifies the C-O-C vibration. These peaks align with values

reported in the literature [61]. Additionally, new peaks resembling those associated with p- $\beta$ CD, as described in the previous section, are observed, confirming the modification of NC with p- $\beta$ CD.

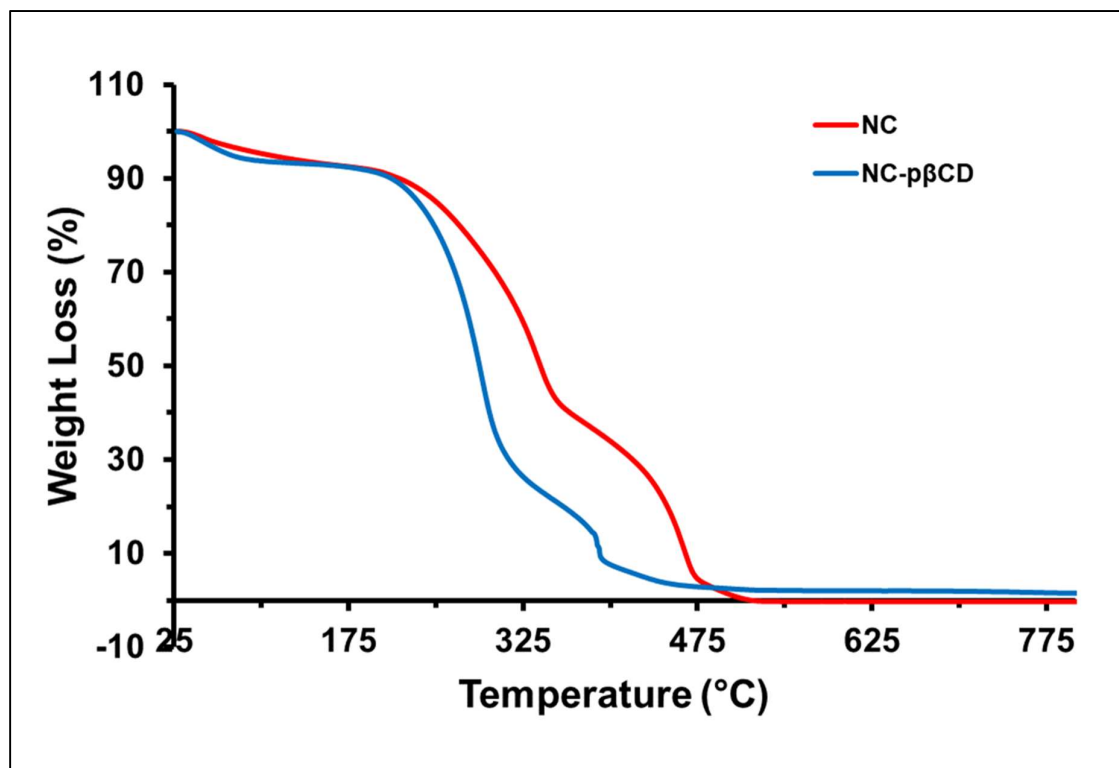


**Figure 3.** Thermogravimetric analysis of NC and NC-p  $\beta$ CD adsorbents.

Furthermore, the TGA technique was employed to study the weight loss of NC and NC-p- $\beta$ CD samples at different temperature ranges, as depicted in Figure 3. The weight loss analysis revealed an initial weight loss of approximately 10% in NC and NC-p- $\beta$ CD samples at temperatures ranging from 25 °C to 225 °C, primarily attributed to moisture loss. Subsequently, a weight loss of around 65% occurred from 225 °C to 320 °C, which can be attributed to hemiacetal loss [62]. The total weight loss reached 98% at 495 °C, resulting from the decomposition of the polymer backbone as well as loss of moisture and hemiacetal. However, the NC-p- $\beta$ CD sample exhibited enhanced thermal stability, with a similar weight loss occurring at a higher temperature of 672 °C, indicating the positive effect of p- $\beta$ CD modification on thermal stability.

The surface morphology and elemental composition of NC and NC-p- $\beta$ CD were further characterized by SEM and EDS. Figure 4 illustrates the SEM images of NC and NC-p- $\beta$ CD, revealing a notable difference in their surface morphology. As depicted in Figure 4a, NC displayed a more agglomerated structure than NC-p- $\beta$ CD (Figure 4b). Conversely, the SEM image of NC-p- $\beta$ CD (Figure 4b) displayed a porous and cleaner structure with petal-like fragments, indicating the structural changes resulting from the modification of NC with p- $\beta$ CD.

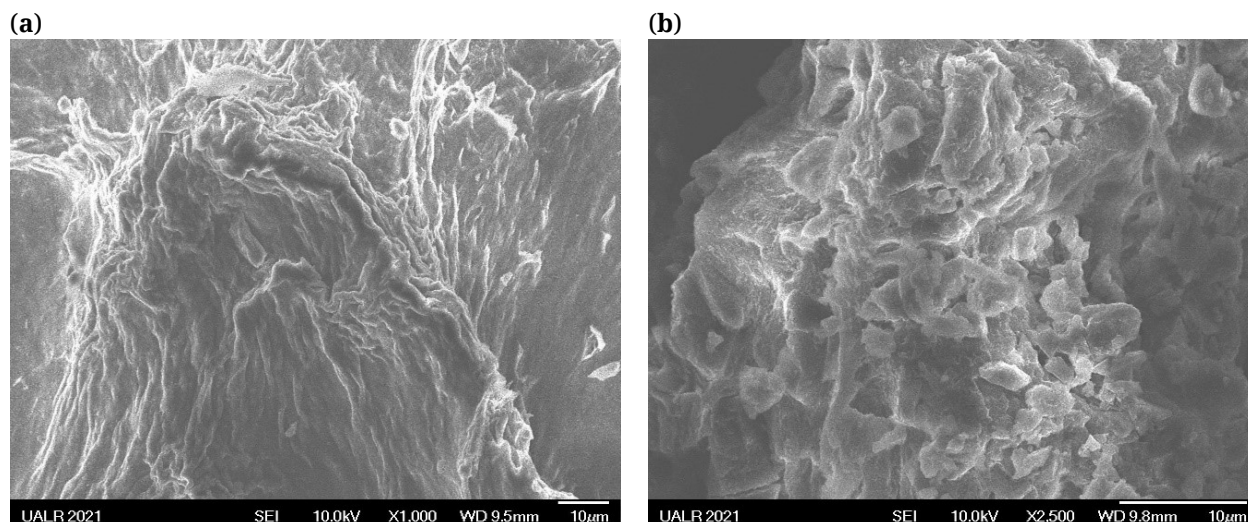


**Figure 4.** SEM images of (a) NC and (b) NC-p- $\beta$ CD adsorbents with their magnifications of  $\times 1000$  and  $\times 2500$ , respectively.

EDS analysis offers valuable insights into the covalent modification of NC with p- $\beta$ CD. Supplementary Figure S4 in the Supplementary Information displays the EDS analysis results for NC and NC-p- $\beta$ CD. The analysis reveals that NC comprises 39.5% carbon and 58.7% oxygen. Following the modification of NC with p- $\beta$ CD, the carbon and oxygen content in NC-p- $\beta$ CD were measured to be 37.5% and 57.6%, respectively. The difference in percentage can be attributed to the modification process from NC to NC-p- $\beta$ CD. Importantly, the variation in the C/O ratios falls within the standard errors of the EDS measurements for these samples, further supporting the reliability of the analysis.

After synthesizing the materials, we evaluated the effectiveness of NC-p- $\beta$ CD in removing BPS, TCS, and TCP. These impurities are hydrophobic and known to pose significant health risks, including endocrine disruption. By incorporating p- $\beta$ CD into NC, we took advantage of the hydrophobic internal cavity of  $\beta$ CD, enabling the entrapment of these impurities within the hydrophobic p- $\beta$ CD ring of NC-p- $\beta$ CD [63]. Moreover, NC offers several advantages, such as a large surface area and numerous hydroxyl groups capable of forming hydrogen bonds [64]. These properties facilitate the adsorption and removal of pollutants by enabling hydrogen bonding on the surface of NC [65]. Additionally, NC is readily available and cost-effective, making it an ideal candidate for developing economically viable filtration materials for pollutant removal [64].

UV-visible spectroscopy was employed to determine the concentration of BPS before and after adsorption onto the adsorbents. Initially, the molar absorptivity coefficient of BPS was calculated by plotting the maximum absorbance against various BPS concentrations, as depicted in Supplementary Figure S5 (Supplementary Information). The calculated molar absorptivity coefficient was determined to be  $2550 \pm 102 \text{ M}^{-1}\text{cm}^{-1}$  at 279 nm.

Figure 5a presents the UV-visible spectra of a  $10^{-4}$  M BPS solution and the spectra obtained after passing 4 mL of the same BPS solution through a filtration plug comprising 100 mg of NC and NC-p- $\beta$ CD respectively, at pH 9. The maximum absorbance of BPS was observed at 268 nm. However, upon passing through the samples, the  $\lambda_{\max}$  shifted to 277 nm, and the absorbance decreased from 1.7 to 0.7 when using only NC as the filtration matrix. Notably, the adsorption dramatically dropped to 0.35 when NC-p- $\beta$ CD was utilized as the filtration matrix. These results indicate that both NC and NC-p- $\beta$ CD effectively remove BPS, with NC-p- $\beta$ CD demonstrating superior adsorption capabilities compared to NC alone.

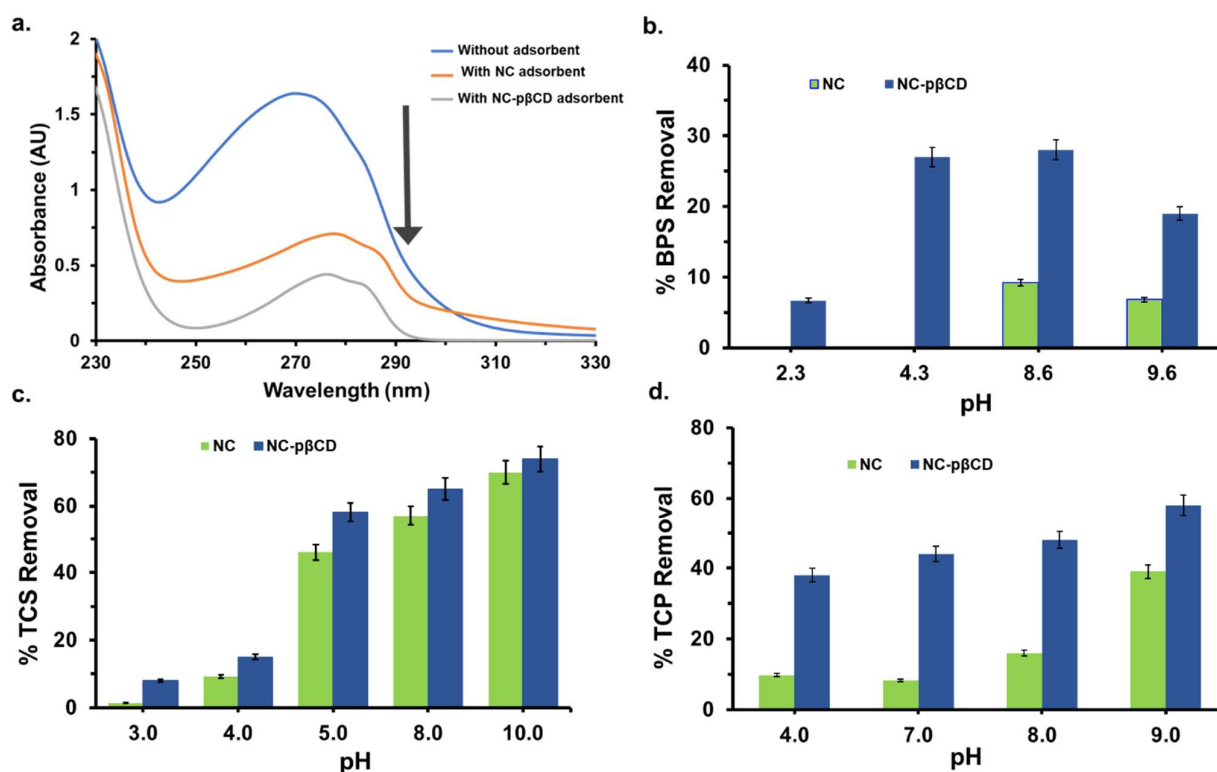


**Figure 5.** (a) UV-visible spectroscopy showing the concentration BPS before passing through the adsorbent (blue line) and after passing through 100 mg of each adsorbent NC (orange line) and NC-p- $\beta$ CD (light green line) separately. Percentage (%) removal of (b) 4 mL  $10^{-4}$  M BPS, (c) 2 mL of  $2 \times 10^{-3}$  M TCS, and (d) 2 mL of  $2 \times 10^{-3}$  M TCP using 100 mg of NC-p- $\beta$ CD adsorbent at different pHs.

The influence of pH on the adsorption properties was further investigated, considering the presence of different functional groups in wastewater impurities. Notably, BPS contains ionizable phenolic groups, highlighting the significance of pH in understanding the adsorption behavior of BPS and other pollutants on NC-p- $\beta$ CD. Figure 5b illustrates the removal percentage of BPS ( $10^{-4}$  M) across a pH range of 2–10. The experiment was conducted using 100 mg of NC and NC-p- $\beta$ CD adsorbents separately at various pH levels.

At low pH values, the adsorption of BPS was minimal, with only 6.7% adsorption at pH 2. Notably, NC exhibited negligible adsorption at this pH. However, at pH 4.3, NC-p- $\beta$ CD demonstrated 27% adsorption, while no significant adsorption was observed using NC alone. This observation suggests that BPS adsorption occurs through host-guest interactions at this pH. As the pH increased to 8.6, the adsorption of BPS by NC-p- $\beta$ CD reached 28% but decreased to 19% at pH 9.6. NC also exhibited some adsorption at pH 8.6 and 9.6, albeit at a lower percentage. The decrease in adsorption capacity of NC-p- $\beta$ CD at pH 9.6 can be attributed to the deprotonation of the phenolic group of BPS, which occurs at the pKa value of BPS (7.42–8.3) [66]. Deprotonation of BPS leads to negative charges on the surface if pH is greater than pKa, resulting in reduced adsorption via host-guest interactions. The maximum removal percentages of BPS on NC-p- $\beta$ CD and NC were found to be 9.2% and 28%, respectively, at pH 8.6.

We conducted additional tests to evaluate the removal efficiency of TCS and TCP using the NC-p- $\beta$ CD adsorbent. Figure 5c illustrates the percentage removal of  $10^{-3}$  M TCS at pH values ranging from 2 to 10, using 100 mg of control (NC) and sample (NC-p- $\beta$ CD) separately. The plot reveals a similar adsorption trend for TCS as observed for BPS. The adsorption of TCS increased with an elevation in pH. Considering the pKa value of TCS (7.9–8.1) [67], deprotonation occurs when pH exceeds the pKa value. This leads to enhanced ion-ion interactions in addition to hydrophobic interactions, resulting in increased adsorption.

Similarly, Figure 5d displays the percentage removal of TCP at different pH levels using 100 mg of control (NC) and sample (NC-p- $\beta$ CD). The graph demonstrates that adsorption also increased with rising pH, resembling the behavior observed for TCS removal. The pKa value of TCP is 6.3, and an increase in pH promotes ion-ion interactions between TCP and NC-p- $\beta$ CD [68]. The maximum percentage removal of TCP was achieved at pH 9 (58%) using NC-p- $\beta$ CD, compared to 39% with NC alone. This indicates that NC-p- $\beta$ CD is effective in removing chlorinated phenols as well.

To investigate the kinetics of the adsorption process, we examined the adsorption of BPS by passing a  $10^{-3}$  M solution (pH 9.0) through NC-p- $\beta$ CD with varying amounts ranging from 10 to 50 mg. The percentage removal of BPS corresponding to different amounts of adsorbent material is presented in Figure 6a. Initially, the adsorption of BPS was limited, but it gradually increased linearly as the quantity of adsorbent material was increased.

We conducted further investigations on the adsorption of TCS by passing a 2 mL solution of  $2 \times 10^{-3}$  M TCS at pH 8.5 through different quantities of NC-p- $\beta$ CD samples, ranging from 10 to 100 mg. The resulting percentage removal of TCS was plotted against the amount of NC-p- $\beta$ CD, as illustrated in Figure 6b.

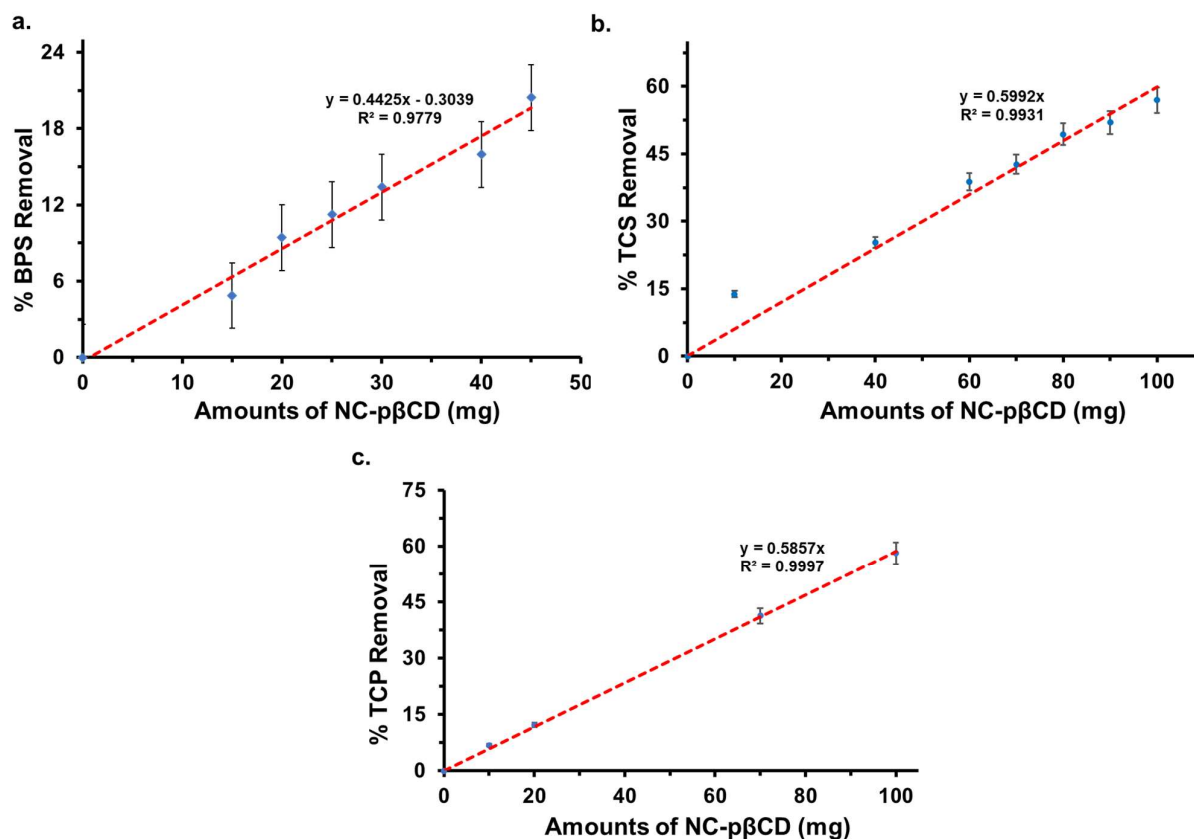


**Figure 6.** Percentage (%) removal of (a) 4 mL of  $10^{-3}$  M BPS at pH 9.0, (b) 2 mL of  $2 \times 10^{-3}$  M TCS at pH 8.5, and (c) 2 mL of  $2 \times 10^{-3}$  M TCP at pH 8.5 using different doses of NC-pβCD.

Similarly, the adsorption of TCP was examined by passing a 2 mL solution of  $2 \times 10^{-3}$  M TCP (pH 8.5) through varying amounts of NC-p-βCD samples, ranging from 10 to 100 mg. Initially, the adsorption of TCP was relatively low, but it increased proportionally with the quantity of adsorbent material, as shown in the corresponding graph depicted in Figure 6c. Notably, the maximum percentage (%) removal of TCP reached 58% when passed through 100 mg of NC-pβCD.

The kinetics of impurity removal from NC-p-βCD were investigated by analyzing both Freundlich and Langmuir adsorption kinetics plots. The Freundlich adsorption kinetics were examined using the equation [69]:

$$\text{Log } q_e = \text{Log } K_f + \frac{1}{n} \text{Log } C_e \quad (\text{i})$$

In this equation,  $q_e$  represents the amount of solute adsorbed per unit adsorbent,  $K_f$  is the Freundlich constant,  $1/n$  is the measure of the intensity of adsorption, and  $C_e$  is the equilibrium concentration of adsorbate.

To assess the Freundlich adsorption kinetics of BPS, TCS, and TCP removal, a plot of  $\log q_e$  against  $\log C_e$  was generated, as depicted in Supplementary Figure S6 (Supplementary Information). However, no linear relationship was observed, indicating that the removal of these impurities did not follow Freundlich's adsorption kinetics [68].

On the other hand, the Langmuir adsorption kinetics were investigated using the following equation (ii) [70].

$$\frac{1}{q_e} = \frac{1}{C_e} \left( \frac{1}{q_o b} \right) + \frac{1}{q_o} \quad (\text{ii})$$

In this equation,  $b$  represents the Langmuir adsorption constant,  $q_o$  is the maximum adsorption capacity,  $q_e$  is the amount of adsorbate adsorbed on the surface of the adsorbent at equilibrium, and  $C_e$  represents the equilibrium concentration of adsorbate.

Figure 7a illustrates the plot of  $1/q_e$  against  $1/C_e$  for BPS adsorption on the surface of NC-p- $\beta$ CD per unit mass at equilibrium (mg/g) [69]. A linear relationship was observed, indicating that the amount of BPS adsorbed depends on the quantity of adsorbent used. This finding supports the conclusion that the adsorption of BPS on NC-p- $\beta$ CD follows Langmuir adsorption kinetics [68].

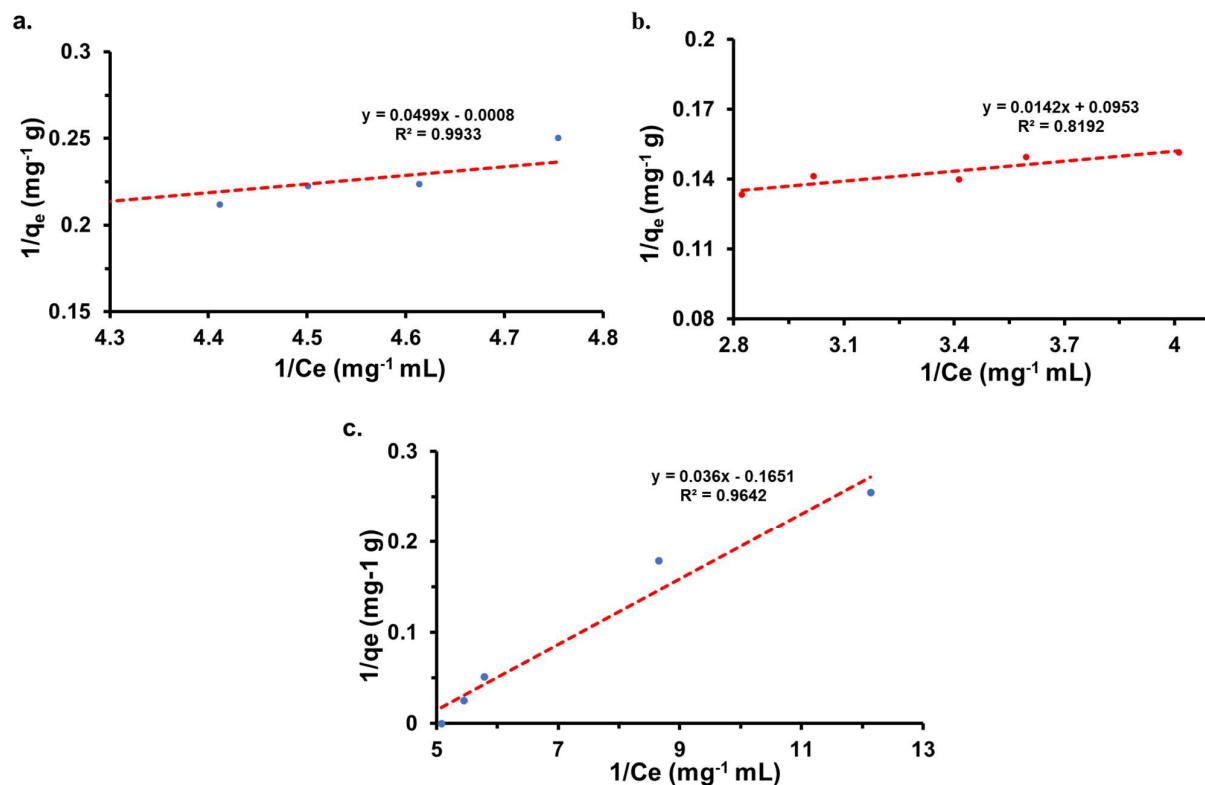


**Figure 7.** Langmuir adsorption kinetics of (a)  $10^{-3}$  M BPS (b)  $2 \times 10^{-3}$  M TCS, and (c)  $2 \times 10^{-3}$  M TCP removal using 100 mg of NC-p- $\beta$ CD adsorbent.

The Langmuir adsorption kinetics of TCS at pH 8.5 using the NC-p- $\beta$ CD adsorbent were investigated by plotting  $1/q_e$  against  $1/C_e$ , as illustrated in Figure 7b. The obtained linear plot suggests that the adsorption of TCS on NC-p- $\beta$ CD followed Langmuir adsorption kinetics [71]. Similarly, the adsorption kinetics of  $2 \times 10^{-3}$  M TCP from the NC-p- $\beta$ CD adsorbent were

studied using Langmuir adsorption kinetics plots, and it also exhibited Langmuir adsorption kinetics, as depicted in Figure 7c.

The recyclability of the NC-p- $\beta$ CD adsorbent was evaluated to assess its adsorption efficacy. The recyclability test was conducted using 100 mg of NC-p- $\beta$ CD adsorbent for four different cycles, and the results are presented in Supplementary Figure S7 (Supplementary Information). Initially, the percentage (%) removal of BPS was high, approximately 30% in the first cycle. However, it gradually decreased to 23%, 21%, and 15% in the second, third, and fourth cycles.

## CONCLUSION

The manuscript presents a successful synthesis and application of a hydrogel material, NC-p- $\beta$ CD. The synthesis was verified using various spectroscopic and microscopic techniques, including FTIR, NMR, TGA, SEM, and EDS. The study investigated the efficacy of NC-p- $\beta$ CD in removing endocrine disruptors (BPS, TCS, and TCP) from aqueous solutions at different pH levels. Enhanced removal was observed at higher pH values due to increased interaction between the impurities and the adsorbent surface. Notably, while the control sample (NC) showed no removal of BPS at acidic pH (2.3 and 4.3), NC-p- $\beta$ CD exhibited effective removal even at low pH. Adsorption kinetics followed Langmuir plots, suggesting monolayer adsorption. Adsorption efficiency was calculated by determining the adsorbed pollutant amount (in mg) per unit milligram of adsorbent. This manuscript showcases the potential of the NC-based hydrogel material, particularly NC-p- $\beta$ CD, for the efficient removal of hydrophobic pollutants. The findings shed light on the pH-dependent adsorption process and offer valuable insights into the kinetics and efficiency of the modified material. These results contribute to the development of environmentally friendly approaches for water pollution remediation. Moving forward, our research endeavors will encompass the broader objective of employing synthesized NC-p- $\beta$ CD materials to eliminate a wider array of impurities. Additionally, we intend to assess the suitability of these materials for biomedical purposes, such as their potential applications in wound healing and tissue engineering.

## SUPPLEMENTARY MATERIALS

The following supplementary materials are available online at <https://doi.org/10.20900/jsr20230010>. Supplementary Figure S1: FTIR spectroscopy of  $\beta$ CD and p- $\beta$ CD samples. Supplementary Figure S2:  $^1\text{H-NMR}$  spectroscopy of p- $\beta$ CD sample. Supplementary Figure S3: FTIR spectroscopy of NC and NC-p- $\beta$ CD adsorbents. Supplementary Figure S4: EDS analysis of (a) NC and (b) NC-p- $\beta$ CD adsorbents. Supplementary Figure S5: Absorbance vs concentration plot of BPS for molar extinction coefficient determination. Supplementary Figure S6: Freundlich adsorption kinetics of (a)  $10^{-3}$  M BPS (b)  $2 \times 10^{-3}$  M TCS, and (c)  $2 \times 10^{-3}$  M TCP removal using 100 mg of NC-p- $\beta$ CD adsorbent. Supplementary Figure

S7: Reusability test of NC-p- $\beta$ CD adsorbent for the removal of  $10^{-4}$  M BPS solution.

#### DATA AVAILABILITY

All data generated from the study are available in the manuscript or in the supplementary data.

#### AUTHOR CONTRIBUTIONS

HP, ABR, SEB, AG (Ahona Ghosh), and FW contributed to the experimental work and data interpretation. AG (Anindya Ghosh) conceived the study and experimental design. HP, ABR, and AG (Anindya Ghosh) were involved in the experimental design and manuscript writing. All authors critically reviewed and approved the final version of the manuscript.

#### CONFLICTS OF INTEREST

The authors declare no competing financial interest. The authors declare no conflicts of interest. The authors are responsible for the content and writing of this article.

#### ACKNOWLEDGMENTS

Anindya Ghosh gratefully acknowledges the financial assistance provided by the AR INBRE grant number GR013696, National Institute of General Medical Sciences (NIGMS) grant number 2P20GM103429-19, and the National Science Foundation Grant No. 2223984 to support this research.

#### REFERENCES

1. Ambika PPS. Natural Polymer-Based Hydrogels for Adsorption Applications. Available from: [https://books.google.com.sg/books?hl=zh-CN&lr=&id=16DgDwAAQBAJ&oi=fnd&pg=PA267&ots=C86-q47tG7&sig=TkNjjkx\\_NqZbSWTgGkjinHDJ7uA#v=onepage&q&f=false](https://books.google.com.sg/books?hl=zh-CN&lr=&id=16DgDwAAQBAJ&oi=fnd&pg=PA267&ots=C86-q47tG7&sig=TkNjjkx_NqZbSWTgGkjinHDJ7uA#v=onepage&q&f=false). Accessed 2023 Aug 25.
2. Gopakumar DA, Arumughan V, Pasquini D, Leu SY, Abdul Khalil HPS, Thomas S. Nanocellulose-Based Membranes for Water Purification. Available from: <https://www.sciencedirect.com/science/article/abs/pii/B9780128139264000045>. Accessed 2023 Aug 25.
3. Manisalidis I, Stavropoulou E, Stavropoulos A, Bezirtzoglou E. Environmental and Health Impacts of Air Pollution: A Review. *Front Public Health*. 2020;8:14.
4. Kurwadkar S, Kanel SR, Nakarmi A. Groundwater Pollution: Occurrence, Detection, and Remediation of Organic and Inorganic Pollutants. *Water Environ Res*. 2020;92(10):1659-68.
5. Khan S, Naushad M, Govarathanan M, Iqbal J, Alfadul SM. Emerging Contaminants of High Concern for the Environment: Current Trends and Future Research. *Environ Res*. 2022;207:112609.
6. Sharma S, Bhattacharya A. Drinking Water Contamination and Treatment

- Techniques. *Appl Water Sci.* 2017;7(3):1043-67.
7. Chowdhury S, Khan N, Kim GH, Harris J, Longhurst P, Bolan NS. Chapter 22—Zeolite for Nutrient Stripping From Farm Effluents. Available from: <https://www.sciencedirect.com/science/article/abs/pii/B9780128038376000226>. Accessed 2023 Aug 25.
  8. Poudel BR, Aryal RL, Bhattarai S, Koirala AR, Gautam SK, Ghimire KN, et al. Agro-Waste Derived Biomass Impregnated with TiO<sub>2</sub> as a Potential Adsorbent for Removal of As(III) from Water. *Catalysts.* 2020;10(10):1125.
  9. Lim S, Yoon JH. Exposure to Environmental Pollutants and a Marker of Early Kidney Injury in the General Population: Results of a Nationally Representative Cross-Sectional Study Based on the Korean National Environmental Health Survey (KoNEHS) 2012–2014. *Sci Total Environ.* 2019;681:175-82.
  10. Kataria A, Trasande L, Trachtman H. The Effects of Environmental Chemicals on Renal Function. *Nat Rev Nephrol.* 2015;11(10):610-25.
  11. Sinha V, Chakma S. Advances in the Preparation of Hydrogel for Wastewater Treatment: A Concise Review. *J Environ Chem Eng.* 2019;7(5):103295.
  12. Thomas Zoeller R, Brown TR, Doan LL, Gore AC, Skakkebaek NE, Soto AM, et al. Endocrine-Disrupting Chemicals and Public Health Protection: A Statement of Principles from The Endocrine Society. *Endocrinology.* 2012;153(9):4097-110.
  13. Bergman Å, Heindel JJ, Kasten T, Kidd KA, Jobling S, Neira M, et al. The Impact of Endocrine Disruption: A Consensus Statement on the State of the Science. *Environ Health Perspect.* 2013;121(4):a104-6.
  14. Varaprasad K, Raghavendra GM, Jayaramudu T, Yallapu MM, Sadiku R. A Mini Review on Hydrogels Classification and Recent Developments in Miscellaneous Applications. *Mater Sci Eng C.* 2017;79:958-71.
  15. World Health Organization. State of the Science of Endocrine Disrupting Chemicals 2012. Available from: <https://www.who.int/publications/i/item/9789241505031>. Accessed 2023 Aug 25.
  16. Liao C, Liu F, Kannan K. Bisphenol S, a New Bisphenol Analogue, in Paper Products and Currency Bills and Its Association with Bisphenol A Residues. *Environ Sci Technol.* 2012;46(12):6515-22.
  17. Li J, Wang Y, Li N, He Y, Xiao H, Fang D, et al. Toxic Effects of Bisphenol A and Bisphenol S on *Chlorella Pyrenoidosa* Under Single and Combined Action. *Int J Environ Res Public Health.* 2022;19(7):4245.
  18. Zheng C, Liu J, Ren J, Shen J, Fan J, Xi R, et al. Occurrence, Distribution and Ecological Risk of Bisphenol Analogues in the Surface Water from a Water Diversion Project in Nanjing, China. *Int J Environ Res Public Health.* 2019;16(18):3296.
  19. Nejumal KK, Dineep D, Mohan M, Krishnan KP, Aravind UK. Aravindakumar CT. Presence of Bisphenol S and Surfactants in the Sediments of Kongsfjorden: A Negative Impact of Human Activities in Arctic? *Environ Monit Assess.* 2018;190(1):22.
  20. Rochester JR, Bolden AL. A Systematic Review and Comparison of the Hormonal Activity of Bisphenol A Substitutes. *Environ Health Perspect.*

- 2015;123(7):643-50.
21. Ben-Jonathan N, Hugo ER. Bisphenols Come in Different Flavors: Is "S" Better Than "A"? *Endocrinology*. 2016;157(4):1321-3.
  22. Winkler J, Liu P, Phong K, Hinrichs JH, Ataii N, Williams K, et al. Bisphenol A Replacement Chemicals, BPF and BPS, Induce Protumorigenic Changes in Human Mammary Gland Organoid Morphology and Proteome. Available from: [https://www.researchgate.net/profile/Elin-Hadler-Olsen/publication/359127737\\_Bisphenol\\_A\\_replacement\\_chemicals\\_BPF\\_and\\_BPS\\_induce\\_protumorigenic\\_changes\\_in\\_human\\_mammary\\_gland\\_organoid\\_morphology\\_and\\_proteome/links/6229e79b3c53d31ba4b638c2/Bisphenol-A-replacement-chemicals-BPF-and-BPS-induce-protumorigenic-changes-in-human-mammary-gland-organoid-morphology-and-proteome.pdf](https://www.researchgate.net/profile/Elin-Hadler-Olsen/publication/359127737_Bisphenol_A_replacement_chemicals_BPF_and_BPS_induce_protumorigenic_changes_in_human_mammary_gland_organoid_morphology_and_proteome/links/6229e79b3c53d31ba4b638c2/Bisphenol-A-replacement-chemicals-BPF-and-BPS-induce-protumorigenic-changes-in-human-mammary-gland-organoid-morphology-and-proteome.pdf). Accessed 2023 Aug 25.
  23. Saini M, Singh Y, Arora P, Arora V, Jain K. Implant Biomaterials: A Comprehensive Review. *World J Clin Cases*. 2015;3(1):52-7.
  24. Prasad SS, Rao KM, Reddy PRS, Reddy NS, Rao KSV, Subha MCS. Synthesis and Characterization of Guar Gum-g-Poly (Acrylamidoglycolic Acid) by Redox Initiator. *Indian J Adv Chem Sci*. 2012;1(1):28-32.
  25. Rolfo A, Nuzzo AM, De Amicis R, Moretti L, Bertoli S, Leone A. Fetal–Maternal Exposure to Endocrine Disruptors: Correlation with Diet Intake and Pregnancy Outcomes. *Nutrients*. 2020;12(6):1744.
  26. Freeman S. Plastic Food Contact Articles—Food Chemical Safety Unwrapped. *Environ Health Rev*. 2018;61(4):92-7.
  27. Thoene M, Dzika E, Gonkowski S, Wojtkiewicz J. Bisphenol S in Food Causes Hormonal and Obesogenic Effects Comparable to or Worse than Bisphenol A: A Literature Review. *Nutrients*. 2020;12(2):532.
  28. Cimmino I, Fiory F, Perruolo G, Miele C, Beguinot F, Formisano P, et al. Potential Mechanisms of Bisphenol A (BPA) Contributing to Human Disease. *Int J Mol Sci*. 2020;21(16):5761.
  29. Ferguson M, Lorenzen-Schmidt I, Pyle WG. Bisphenol S Rapidly Depresses Heart Function Through Estrogen Receptor- $\beta$  and Decreases Phospholamban Phosphorylation in a Sex-Dependent Manner. *Sci Rep*. 2019;9(1):15948.
  30. Liaqat I. Interactions between Bisphenol S or Dibutyl Phthalates and Reproductive System. Available from: <https://web.archive.org/web/20190503123647id /https://cdn.intechopen.com/pdfs/63253.pdf>. Accessed 2023 Aug 25.
  31. Wang R, Fei Q, Liu S, Weng X, Liang H, Wu Y, et al. The Bisphenol F and Bisphenol S and Cardiovascular Disease: Results from NHANES 2013–2016. *Environ Sci Eur*. 2022;34(1):1-10.
  32. Inadera H. Neurological Effects of Bisphenol A and Its Analogues. *Int J Med Sci*. 2015;12(12):926-36.
  33. Song P, Fan K, Tian X, Wen J. Bisphenol S (BPS) Triggers the Migration of Human Non-Small Cell Lung Cancer Cells via Upregulation of TGF- $\beta$ . *Toxicol Vitro*. 2019;54:224-31.
  34. Siddique MAB, Harrison SM, Monahan FJ, Cummins E, Brunton NP. Bisphenol A and Metabolites in Meat and Meat Products: Occurrence, Toxicity, and Recent Development in Analytical Methods. *Foods*. 2021;10(4):714.
  35. Pizzino G, Irrera N, Cucinotta M, Pallio G, Mannino F, Arcoraci V, et al.

- Oxidative Stress: Harms and Benefits for Human Health. *Oxid Med Cell Longev*. 2017;2017:8416763.
36. Rubin BS. Bisphenol A: An Endocrine Disruptor with Widespread Exposure and Multiple Effects. *J Steroid Biochem Mol Biol*. 2011;127(1–2):27-34.
  37. Yueh MF, Tukey RH. Triclosan: A Widespread Environmental Toxicant with Many Biological Effects. *Annu Rev Pharmacol*. 2016;56:251-72.
  38. Weatherly LM, Gosse JA. Triclosan Exposure, Transformation, and Human Health Effects. *J Toxicol Environ Health B Crit Rev*. 2017;20(8):447-69.
  39. Loganathan P, Vigneswaran S, Kandasamy J, Cuprys AK, Maletskyi Z, Ratnaweera H. Treatment Trends and Combined Methods in Removing Pharmaceuticals and Personal Care Products from Wastewater—A Review. *Membranes*. 2023;13(2):158.
  40. Azqhandi MHA, Foroughi M, Yazdankish E. A Highly Effective, Recyclable, and Novel Host-Guest Nanocomposite for Triclosan Removal: A Comprehensive Modeling and Optimization-Based Adsorption Study. *J Colloid Interface Sci*. 2019;551:195-207.
  41. Chu W, Law CK. Treatment of Trichlorophenol by Catalytic Oxidation Process. *Water Res*. 2003;37(10):2339-46.
  42. Ghochlavi N, Aghapour AA. Biodegradation of 2-4-6 Trichlorophenol by Sequencing Batch Reactors (SBR) Equipped with a Rotating Biological Bed and Operated in an Anaerobic-Aerobic Condition. *Front Environ Sci*. 2022;10:1015790.
  43. Su T, Gao W, Gao Y, Ma X, Gao L, Song Y. The Application of Response Surface Methodology for 2,4,6-Trichlorophenol Removal from Aqueous Solution Using Synthesized Zn<sup>2+</sup>-Al<sup>3+</sup>-Tartrate Layered Double Hydroxides. *Processes*. 2022;10(2):282.
  44. Singh DK, Srivastava B. Removal of Phenol Pollutants from Aqueous Solutions Using Various Adsorbents. *J Sci Ind Res*. 2002;61(3):208-18.
  45. Ghasemi Z, Younesi H. Preparation and Characterization of Nanozeolite NaA from Rice Husk at Room Temperature without Organic Additives. *J Nanomater*. 2011;2011:1-8.
  46. Zbair M, Ojala S, Khallok H, Ainassaari K, El Assal Z, Hatim Z, et al. Structured Carbon Foam Derived From Waste Biomass: Application to Endocrine Disruptor Adsorption. *Environ Sci Pollut Res Int*. 2019;26(31):32589-99.
  47. Tisserant A, Cherubini F. Potentials, Limitations, Co-Benefits, and Trade-Offs of Biochar Applications to Soils for Climate Change Mitigation. *Land*. 2019;8(12):179.
  48. Wang J, Man H, Sun L, Zang S. Carbon Black: A Good Adsorbent for Triclosan Removal from Water. *Water*. 2022;14(4):576.
  49. Zhou Y, Xue C, Gan L, Owens G, Chen Z. Simultaneous Removal of Triclosan and Cd(II) by Bio-Reduced Graphene Oxide and Its Mechanism. *Chemosphere*. 2023;311:137021
  50. Krishnaiah D, Anisuzzaman SM, Bono A, Sarbatly R. Adsorption of 2,4,6-trichlorophenol (TCP) onto activated carbon. *J King Saud Univ Sci*. 2013;25(3):251-5.
  51. Jabeen A, Kamran U, Noreen S, Park S, Bhatti HN. Mango Seed-Derived Hybrid

- Composites and Sodium Alginate Beads for the Efficient Uptake of 2,4,6-Trichlorophenol from Simulated Wastewater. *Catalysts*. 2022;12(9):972.
52. RanguMagar AB, Chhetri BP, Parnell CM, Parameswaran-Thankam A, Watanabe F, Mustafa T, et al. Removal of Nitrophenols From Water Using Cellulose Derived Nitrogen Doped Graphitic Carbon Material Containing Titanium Dioxide. *Part Sci Technol*. 2019;37(4):444-52.
  53. Yempally S, Hegazy SM, Aly A, Kannan K, Sadasivuni KK. Non-Invasive Diabetic Sensor Based on Cellulose Acetate/Graphene Nanocomposite. *Macromol Symp*. 2020;392(1):2000024.
  54. Ansari JR, Hegazy SM, Houkan MT, Kannan K, Aly A, Sadasivuni KK. Nanocellulose-based materials/composites for sensors. Available from: <https://www.sciencedirect.com/science/article/abs/pii/B9780128223505000084>. Accessed 2023 Aug 25.
  55. Kumar NS, Asif M, Poulouse AM, Suguna M, Al-Hazza MI. Equilibrium and Kinetic Studies of Biosorptive Removal of 2,4,6-Trichlorophenol from Aqueous Solutions Using Untreated Agro-Waste Pine Cone Biomass. *Processes*. 2019;7(10):757.
  56. Zou L, Mi C, Yu H, Gu W, Teng Y. Characterization of the Interaction Between Triclosan and Catalase. *RSC Adv*. 2017;7:9031-6.
  57. Fu D, Zhang Q, Chen P, Zheng X, Hao J, Mo P, et al. Efficient Removal of Bisphenol Pollutants on Imine-Based Covalent Organic Frameworks: Adsorption Behavior and Mechanism. *RSC Adv*. 2021;11:18308-20.
  58. Gidwani B., Vyas A. Synthesis, Characterization and Application of Epichlorohydrin-Cyclodextrin Polymer. *Colloids Surf B*. 2014;114:130-7.
  59. Rachmawati H, Edityaningrum CA, Mauludin R. Molecular Inclusion Complex of Curcumin- $\beta$ -Cyclodextrin Nanoparticle to Enhance Curcumin Skin Permeability from Hydrophilic Matrix Gel. *Aaps Pharmscitech*. 2013;14(4):1303-12.
  60. Sambasevam KP, Mohamad S, Sarih NM, Ismail NA. Synthesis and Characterization of the Inclusion Complex of  $\beta$ -Cyclodextrin and Azomethine. *Int J Mol Sci*. 2013;14(2):3671-82.
  61. Vibhore AB, Rastogi VK, Mahurm BK, Rastogi A, Abdel-Haleem FM, Samyn P. Nanocelluloses as New Generation Materials: Natural Resources, Structure-Related Properties, Engineering Nanostructures, and Technical Challenges. *Mater Today Chem*. 2022;26(1):101247.
  62. Yang H, Yan R, Chen H, Lee DH, Zheng C. Characteristics of Hemicellulose, Cellulose and Lignin Pyrolysis. *Fuel*. 2007;86(12-13):1781-8.
  63. Lebedinskiy K, Lobaz V, Jindřich J. Preparation of  $\beta$ -Cyclodextrin-Based Dimers with Selectively Methylated Rims and Their Use For Solubilization of Tetracene. *Beilstein J Org Chem*. 2022;18(1):1596-606.
  64. Ahankari S, George T, Subhedar A, Kar KK. Nanocellulose as a Sustainable Material for Water Purification. *SPE Polym*. 2020;1(2):69-80.
  65. George J, Sabapathi SN. Cellulose Nanocrystals: Synthesis, Functional Properties, and Applications. *Nanotechnol Sci Appl*. 2015;8:45-54.
  66. Regueiro J, Breidbach A, Wenzl T. Derivatization of Bisphenol A and Its Analogues with Pyridine-3-Sulfonyl Chloride: Multivariate Optimization and

- Fragmentation Patterns by Liquid Chromatography/Orbitrap Mass Spectrometry. *Rapid Commun Mass Spectrom.* 2015;29(16):1473-84.
67. Lyndall J, Fuchsman P, Bock M, Barber T, Lauren D, Leigh K, et al. Probabilistic Risk Evaluation for Triclosan in Surface Water, Sediments, and Aquatic Biota Tissues. *Integr Environ Assess Manag.* 2010;6(3):419-40.
68. Kumar NS, Asif M, Al-Hazzaa MI, Ibrahim AA. Biosorption of 2,4,6-Trichlorophenol From Aqueous Medium Using Agro-Waste: Pine (*Pinus densiflora* Sieb) Bark Powder. *Acta Chim Solv.* 2018;65(1):221-30.
69. Said KAM, Ismail NZ, Jama'in RL, Alipah NAM, Sutan NM, Gadung GG, et al. Application of Freundlich and Temkin Isotherm to Study the Removal of Pb(II) Via Adsorption on Activated Carbon Equipped Polysulfone Membrane. *Int J Eng Technol.* 2018;7(18):913.
70. Gedam AH, Dongre RS. Pb (II) Ions Adsorption onto Biomaterial Chitosan Hydrogel Beads—Isotherm and Kinetic Studies. Available from: [https://www.researchgate.net/profile/Rajendra-Dongre/publication/318673312\\_Pb\\_II\\_Ions\\_Adsorption\\_onto\\_Biomaterial\\_Chitosan\\_Hydrogel\\_Beads\\_-\\_Isotherm\\_And\\_Kinetic\\_Studies/links/597712c0aca2728d0276fad0/Pb-II-Ions-Adsorption-onto-Biomaterial-Chitosan-Hydrogel-Beads-Isotherm-And-Kinetic-Studies.pdf](https://www.researchgate.net/profile/Rajendra-Dongre/publication/318673312_Pb_II_Ions_Adsorption_onto_Biomaterial_Chitosan_Hydrogel_Beads_-_Isotherm_And_Kinetic_Studies/links/597712c0aca2728d0276fad0/Pb-II-Ions-Adsorption-onto-Biomaterial-Chitosan-Hydrogel-Beads-Isotherm-And-Kinetic-Studies.pdf). Accessed 2023 Aug 25.
71. Islam MA, Chowdhury MA, Mozumder MSI, Uddin MT. Langmuir Adsorption Kinetics in Liquid Media: Interface Reaction Model. *ACS Omega.* 2021;6(22):14481-92.

How to cite this article:

Poudel H, RanguMagar AB, Ghosh A, Bourdo SE, Watanabe F, Wang D, et al. Poly- $\beta$ -Cyclodextrin Functionalized Nanocellulose for Efficient Removal of Endocrine Disrupting Chemicals. *J Sustain Res.* 2023;5(3):e230010. <https://doi.org/10.20900/jsr20230010>